



Communication

Influence of the Physico-Chemical Properties of Model Compounds on the Mean Sizes and Retention Rate of Gliadin Nanoparticles

Silvia Voci, Massimo Fresta and Donato Cosco *

Department of Health Sciences, Campus Universitario “S. Venuta”, University “Magna Græcia” of Catanzaro, I-88100 Catanzaro, Italy; silvia.voci@studenti.unicz.it (S.V.); fresta@unicz.it (M.F.)

* Correspondence: donatocosco@unicz.it; Tel.: +39-0961-369-4119

Abstract: Vegetal proteins have emerged as appealing starting materials for the development of various drug delivery systems, and their use for obtaining polymeric nanoparticles has been profitably exploited in multidisciplinary fields. Wheat gliadin, the water-insoluble storage protein of gluten, is characterized by a great amount of hydrophobic amino acid residues and notable mucoadhesive features. This biopolymer can be easily manipulated to form colloidal carriers, films and fibers by means of bio-acceptable solvents and easy preparation procedures. In this investigation, four model compounds characterized by different octanol/water partition coefficient (logP) values were encapsulated in gliadin nanoparticles, with the aim of investigating the influence of their physico-chemical properties on the cargo features and technological characteristics of the protein nanocarriers. The results demonstrate that the chemical structure, solubility and molecular weight of the compounds used are able to dramatically modulate the mean sizes and the entrapment efficiency of gliadin nanoparticles. This demonstrates the importance of a preformulation investigation when a molecule needs to be encapsulated in this type of polymeric carrier.

Keywords: drug delivery; gliadin; polymeric nanoparticles; vegetal proteins



Citation: Voci, S.; Fresta, M.; Cosco, D. Influence of the Physico-Chemical Properties of Model Compounds on the Mean Sizes and Retention Rate of Gliadin Nanoparticles.

Nanomanufacturing **2021**, *1*, 160–170.

<https://doi.org/10.3390/nanomanufacturing1030011>

Academic Editor: Andres Castellanos-Gomez

Received: 27 October 2021

Accepted: 16 November 2021

Published: 19 November 2021

Publisher’s Note: MDPI stays neutral with regard to jurisdictional claims in published maps and institutional affiliations.



Copyright: © 2021 by the authors. Licensee MDPI, Basel, Switzerland. This article is an open access article distributed under the terms and conditions of the Creative Commons Attribution (CC BY) license (<https://creativecommons.org/licenses/by/4.0/>).

1. Introduction

The concept of the nanoencapsulation of a compound in drug delivery systems has unlocked new opportunities in various fields of application because it has greatly improved the efficacy and safety of many bioactives [1–4]. Over the years, the exploitation of polymeric nanoparticles has shown great potential for biomedical, pharmaceutical and food purposes [5–7]. Various raw materials and techniques have been proposed for the development of nanoparticles and among these the nanoprecipitation of vegetal proteins was used to obtain nanosystems characterized by the scale-up feasibility, great biocompatibility/biodegradability and high entrapment efficiency of several molecules [8–11].

One of the great advantages of these raw materials is the presence of different functional groups able to promote interaction with both hydrophilic and lipophilic compounds, as well as the decoration of the surface of the resulting formulations with different ligands, without the need for any chemical refinement [12–14].

The degree of hydrophilicity or lipophilicity of a bioactive is commonly expressed by the *n*-octanol/water partition coefficient (logP), which is used to predict the behavior of the compound in a biological system, with the aim of providing information concerning its adsorption, distribution, metabolism and excretion features [15]. Generally, a logP value of <1 is typical of water-soluble bioactives, whereas an increased lipophilicity is related to higher logP values [16].

Although an optimal logP value has not been reported, a high degree of hydrophilicity can compromise the cell uptake of a compound, whereas molecules that are highly lipophilic can make their administration difficult, especially regarding the intravenous

route because of their poor affinity for polar media [17–19]. Nanotechnology can be exploited to circumvent these drawbacks, because it allows the enhancement of the drug solubility and bioavailability of a compound as a consequence of the peculiar properties of the drug delivery systems [20–22].

The interactions between the material used to obtain the carrier and the entrapped compound are fundamental for obtaining a stable formulation; that is, based on the functional groups occurring in both of the structures involved, their interactions can be driven by hydrogen, hydrophobic, electrostatic, Van der Waals or dipole–dipole bonds [23,24]. To better investigate this aspect, the exploitation of various model compounds is an approach routinely used to obtain information concerning the ability of a formulation to retain and release the payload, as well as to evaluate the *in vivo* biodistribution or *in vitro* uptake of the nanoparticles, as has been reported in several experimental works [25–29].

In this regard, Gupta and coworkers investigated the influence of six antitumor compounds (carboplatin, cisplatin, docetaxel, doxorubicin, 5-fluorouracil and tamoxifen) on the rheological properties of hydrogels made up of a L-alanine derivative (1.5% *w/v*) [23]. Among these, tamoxifen and 5-fluorouracil achieved the best results since they did not affect the mechanical properties of the hydrogels and demonstrated the highest entrapment efficiencies among the compounds analyzed. This was a consequence of multiple non-polar interactions and hydrogen bonds that each drug established with the gelling polymer; furthermore, this evidence highlighted the suitability of the proposed hydrogels as multidrug carriers [23].

In another experimental investigation, poly-lactide-co-glycolide-acid (PLGA) nanoparticles were evaluated as carriers for sodium fluorescein, sulforhodamine and boron-dipyrromethene (BODIPY[®]493/503) used as a model of hydrophilic, amphiphilic and lipophilic drugs, respectively [30]. The greatest entrapment efficiency and loading capacity were observed for BODIPY, and this was attributed to the mutual hydrophobicity that characterized both the probe and the polymer [30].

Recently, our research team investigated the crucial role exerted by the nature of a compound entrapped in gels made up of 20% *w/v* of zein [31]. In particular, it was shown that the rheological features, as well as the leakage profile from the tridimensional network, were modulated by the physico-chemical features of the entrapped molecule. This happened as a consequence of the different interactions occurring between the vegetal protein and the payload, demonstrating the possibility of tailoring the technological properties of the formulation as a function of the required outcome [31].

In the current investigation, four compounds characterized by different logP values were encapsulated in a polymeric matrix made up of gliadin, the storage proline and glutamine-rich protein extracted from wheat grains, in order to evaluate the influence of their physico-chemical properties on the mean sizes of the nanosystems and the retention rate (Figure 1). Specifically, brilliant blue R (BB) and disodium fluorescein (DF), two fluorescent dyes commonly used to mark proteins [32] and to study drug transport in the liver [33], respectively, were used as models of hydrophilic compounds. In addition, rutin and methylene blue (MB), molecules characterized by antioxidant [34] and antibacterial [31] properties, were exploited as amphiphilic and lipophilic model compounds, respectively.

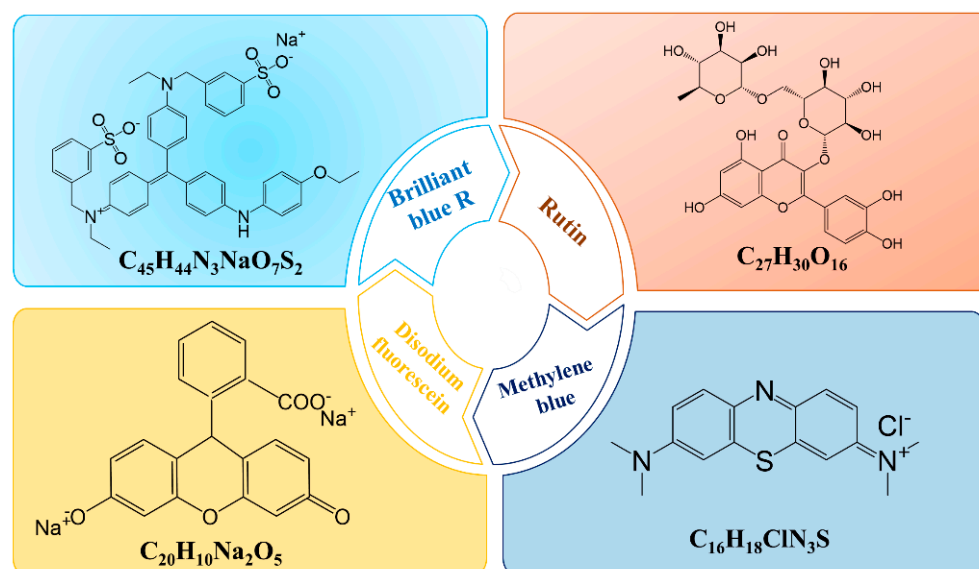


Figure 1. Chemical structures of the model drugs encapsulated in gliadin nanoparticles.

2. Materials and Methods

2.1. Materials

Gliadin from wheat, brilliant blue R (BB), disodium fluorescein (SD), methylene blue (MB) and rutin were purchased from Sigma-Aldrich Co. (St. Louis, MO, USA). Ethanol was supplied from Carlo Erba S.p.A (Rodano, Milan, Italy). Super Refined Brij O2 (SRO2) was obtained from Croda International (Snaith, UK).

2.2. Preparation of Gliadin-Based Nanoparticles Containing Model Compounds

Gliadin nanoparticles were prepared following the nanoprecipitation technique, as previously reported [35]. Namely, 1 mg/mL of gliadin and 0.1% *w/v* of SRO2 were solubilized in 3 mL of a hydroalcoholic solution (Et:H₂O 7:3 *v/v*). The pH of this solution was adjusted to 10, and then 5 mL of MilliQ water were added to this suspension. This mixture was homogenized with an Ultraturrax (model T25 IKA[®] Werke GmbH & Co., Staufen, Germany) at 24,000 rpm for two minutes and then mechanically stirred for 6 h in order to allow the complete evaporation of ethanol [35]. The nanoparticles containing the model compounds were obtained by adding various amounts of each molecule (50, 100, 200 and 400 µg/mL) to the organic or aqueous phase, according to their physico-chemical features (Table 1).

Table 1. Physico-chemical properties of the molecules used as model compounds.

Model Drug	LogP	Molecular Weight (g/mol)	Water Solubility (g/L)	Source
Brilliant blue R (BB)	−0.17	825.97	10	Pubchem/National Diagnostic
Disodium fluorescein (DF)	−0.67	376.30	500	Pubchem/Merck
Methylene blue (MB)	0.75	319.86	43.6	Pubchem
Rutin	0.15	610.50	0.125	Pubchem/Drug Bank

2.3. Physico-Chemical Characterization

The physico-chemical features of the gliadin nanosystems were evaluated by means of dynamic light scattering, using a Zetasizer Nano ZS apparatus (Malvern Panalytical Ltd., Spectris plc, Malvern, UK) applying the third order cumulant correlation function. Each

measurement is the average of three different experiments carried out on three different batches and reported as a function of the intensity (%) \pm the standard deviation [36,37].

2.4. Entrapment Efficiency and Loading Capacity of Model Drugs

The amount of hydrophilic and hydrophobic compounds retained by the gliadin nanoparticles was calculated through spectrophotometric analyses. Namely, 1 mL of formulation containing different amounts of the model drugs (50–400 $\mu\text{g}/\text{mL}$) was centrifuged with a Beckman Optima™ Ultracentrifuge (Fullerton, NU, Canada) at 90,000 rpm for 1 h. The pelletized formulations were freeze-dried in the absence of any cryoprotectant and then incubated for 72 h in water or ethanol based on the physico-chemical features of the entrapped compound. Specifically, the pellet obtained from the BB- and DF-loaded gliadin nanosystems was incubated in water, whereas that obtained from the samples containing MB and rutin was incubated in ethanol. This was done in order to favor the leakage of the entrapped compound [35,38].

The samples were analyzed with a spectrophotometer (Perkin Elmer Lambda 35, Waltham, MA, USA) at a λ_{max} of 490 nm, 590 nm, 359 nm and 663 nm for disodium fluorescein, brilliant blue R, rutin and methylene blue, respectively [31,34]. Empty nanosystems were treated as blank.

The entrapment efficiency (%) was calculated as follows

$$\text{EE}\% = D_E/D_A \times 100 \quad (1)$$

where D_E is the amount of entrapped molecules, and D_A is the amount of compound initially added.

The iodine–iodide assay was used to investigate the amount of SRO2 integrated in the gliadin nanoparticles, as previously reported [38].

The loading capacity (%) was calculated as the percentage ratio between the amount of encapsulated model drug and the total weight of the nanoparticles as follows:

$$\text{LC}\% = [\text{entrapped compound}]/\text{total weight of nanoparticles} \times 100 \quad (2)$$

2.5. Statistical Analysis

The statistical analysis of the various experiments was carried out using a one-way ANOVA. The results were checked using a posteriori Bonferroni t-test with a p value of <0.05 considered statistically significant.

3. Results and Discussion

Recently, the physico-chemical and technological features of gliadin-based nanoparticles have been investigated in order to develop and refine a colloidal formulation that could be useful for various applications. The best results in terms of mean diameter and size distribution were obtained following the nanoprecipitation of 1 mg/mL of protein and 0.1% w/v of SRO2 as stabilizer [35]. The obtained gliadin nanoparticles efficiently retained the hydrophilic compounds, which was surprising because the protein is made up of several lipophilic amino acid residues, and up to now, few examples of a water-soluble compound entrapped within gliadin colloidal systems have been reported [39,40].

In order to gain information concerning the most suitable physico-chemical features that a compound should possess for entrapment within the gliadin nanosystems, four model molecules characterized by different degrees of hydrophilicity/hydrophobicity (Table 1) were investigated as cargo derivatives.

As can be seen in Table 2, the addition of BB during the preparation procedure of the gliadin nanoparticles evidenced the formation of a population characterized by a mean diameter and a PdI of less than 200 nm and 0.3, respectively. While DF showed only a slight increase of these parameters when amounts ≥ 0.1 mg/mL of the compound were used for the preparation of samples. On the contrary, the addition of MB promoted a significant

($p < 0.001$) increase of the mean sizes of the samples when 0.2, and particularly, 0.4 mg/mL of the drug were used. The same trend was observed for their size distribution.

Table 2. Physico-chemical properties of gliadin nanoparticles (1 mg/mL of protein and 0.1% *w/v* of SRO2) prepared with various amounts of model compounds.

Model Drug	Amount of Compound Initially Added (mg/mL)	Mean Sizes (nm)	Polydispersity Index (PDI)
Brilliant blue R (BB)	0.050	154 ± 1	0.176 ± 0.010
	0.100	190 ± 5 **	0.216 ± 0.030 *
	0.200	161 ± 2	0.255 ± 0.040 **
	0.400	150 ± 6	0.284 ± 0.041 **
Disodium fluorescein (DF)	0.050	152 ± 2	0.197 ± 0.008
	0.100	162 ± 8	0.200 ± 0.021
	0.200	170 ± 4 *	0.316 ± 0.024 **
	0.400	208 ± 3 **	0.335 ± 0.006 **
Methylene blue (MB)	0.050	152 ± 1	0.223 ± 0.016 **
	0.100	240 ± 3 **	0.208 ± 0.010 **
	0.200	858 ± 13 **	0.957 ± 0.074 **
	0.400	>1000 **	0.900 ± 0.053 **
Rutin	0.050	215 ± 14 **	0.423 ± 0.058 **
	0.100	180 ± 13	0.417 ± 0.064 **
	0.200	237 ± 14 **	0.466 ± 0.080 **
	0.400	370 ± 73 **	0.491 ± 0.085 **

* $p < 0.05$; ** $p > 0.001$ with respect to the empty nanoformulation.

It should be considered that DF and MB are characterized by a lower molecular weight as compared to BB and, consequently, should provide a lesser degree of steric hindrance and perturbation towards the colloidal architecture (Tables 1 and 2).

However, molecular weight is not the only parameter that should be taken into consideration during a preformulation investigation because the different hydrophilicity/hydrophobicity of the compounds, as well as the presence of specific residues in their structures, play a crucial role in the final rearrangement of gliadin nanoparticles.

Namely, the two sulfonic groups and the three nitrogen moieties occurring in the structure of BB have been demonstrated to promote its interaction with protein polymers, as was true in the case of bovine haemoglobin [41]. In particular, these residues can ensure the formation of multiple hydrogen bonds able to stabilize the polymer-dye complexes and favor the location of BB within the polymeric matrix, as previously reported [41].

It is probable that the absence of the aforementioned residues is a plausible explanation for the destabilizing effect that DF and MB exerted over the assembly of the gliadin nanoparticles (Table 2). In this regard, it was demonstrated that the development of zein microspheres containing promethazine, a phenothiazine derivative with antihistaminic properties and structurally related to MB, exhibited poor retention of the compound as a consequence of the absence of hydrogen bonds between the drug and the vegetal protein [42]. A similar trend has been recently observed using zein-based gels [31].

When the gliadin nanoparticles were prepared following the addition of different amounts of rutin as an amphiphilic model drug, a scarce predisposition of the compound to interact with the polymer was observed. As can be seen in Table 2, a greater mean diameter and a ~3-fold increase in the size distribution of the samples were obtained when just 0.05 mg/mL of drug were used with respect to the empty formulation, and the same trend was observed at higher concentrations of the compound. These results are in disagreement with our recent findings concerning the entrapment of rutin into colloidal carriers made up of zein [34] and can be interpreted as a function of (i) the different aminoacidic composition of the two polymers, with zein being more hydrophobic than gliadin [43,44] and (ii) the

structural organization of the gliadin molecules which consists of an inner hydrophilic core flanked by two hydrophobic regions [45,46].

It is plausible that the encapsulation of rutin into a drug delivery system is mainly driven by Van der Waals and non-polar interactions, as was demonstrated in the case of core shell nanoparticles made up of casein and pectin [47], alumina and titanium dioxide- [48] and human haemoglobin-based nanoparticles [49]. In addition, the steric hindrance exerted by the rutinose moiety discouraged the correct location of the compound within the polymeric matrix, as was true in the case of bovine hemoglobin [50]. Another plausible explanation can be attributed to the low amount of tryptophan residues in the gliadin polymer [51,52], which was demonstrated to be critical for the formation of stable complexes with proteins, as reported in the case of human and bovine serum albumin [53,54] as well as whey proteins [55] and bovine haemoglobin [50].

The entrapment efficiency (EE%) and loading capacity (LC%) are two parameters to be evaluated during the developmental phase of a formulation because they determine its potential use as a drug delivery system [56].

As can be seen in Figure 2 and Table 3, the results concerning these parameters were dramatically influenced by the physico-chemical features and molecular structure of the compound used, and confirmed the trend observed during the DLS analysis. Indeed, only ~5% of rutin became encapsulated in the gliadin nanoparticles when 50 and 100 µg/mL of compound were used, respectively, whereas a decrease in the EE was observed when higher concentrations of the drug were used. A slight increase of this parameter was observed for MB (Figure 2), even though it should be considered that at concentrations ≥ 0.2 mg/mL of the compound a significant polydispersity (PDI > 0.9) of the samples was observed, so the EE and LC of these formulations were not evaluated because they were not stable enough to be analyzed (Table 2).

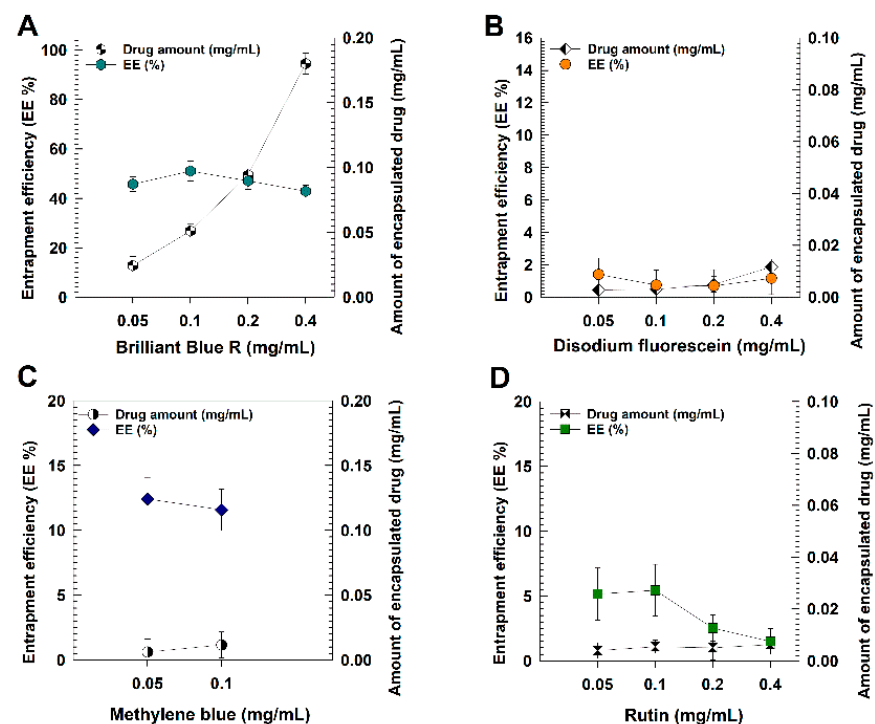


Figure 2. Entrapment efficiency (EE%) of gliadin nanoparticles prepared with 1 mg/mL of protein and 0.1% *w/v* of SRO2. Panel (A): EE% of brilliant blue R. Panel (B): EE% of disodium fluorescein. Panel (C): EE% of methylene blue. Panel (D): EE% of rutin. X-axis: amount of compound (mg/mL) added during the preparation of the samples. Y-axes: percentage of compound entrapped in the gliadin nanoparticles (left); amount of compound (mg/mL) that became entrapped in the gliadin nanoparticles (right).

Table 3. Loading capacity (LC%) of gliadin nanoparticles (1 mg/mL of protein and 0.1% *w/v* of SRO2) prepared with various amounts of model compounds.

Model Compound	Amount of Compound Initially Added (mg/mL)	LC (%)
Brilliant blue R (BB)	0.050	1.79 ± 1.0
	0.100	3.68 ± 0.18
	0.200	6.57 ± 0.33
	0.400	11.87 ± 1.0
Disodium fluorescein (DF)	0.050	0.21 ± 0.0105
	0.100	0.23 ± 0.0115
	0.200	0.37 ± 0.0185
	0.400	0.87 ± 0.004
Methylene blue (MB)	0.050	0.46 ± 0.073
	0.100	0.86 ± 0.043
	0.200	0.19 ± 0.010
	0.400	0.41 ± 0.021
Rutin	0.050	0.37 ± 0.190
	0.100	0.46 ± 0.023
	0.200	1.79 ± 1.0
	0.400	3.68 ± 0.18

The evaluation of the loading capacity confirmed the unsuitability of MB for encapsulation in the gliadin samples because only ~6 and ~12 µg of compound per mg of nanoparticles were retained when 0.05 and 0.1 mg of molecules were added during the preparation procedure. A similar trend was observed for MB-loaded PLGA nanoparticles prepared by the single- and combined- emulsification techniques [57].

The lowest EE and LC values were obtained for the hydrophilic DF, and this confirmed the modest degree of affinity occurring between the biomaterial and this compound (Figure 2 and Table 3). This was surprising because the presence of a carboxylate group and the aromatic moieties in the DF structure should have promoted a great deal of interaction with the gliadin polymer (hydrogen bonds and hydrophobic interactions, respectively). Indeed, these interactions have already been shown to be critical for the interaction of DF with protein polymers, as was true for bovine serum albumin [58] and zein [31].

Moreover, these results are in disagreement with our previous findings in which another xanthene-type dye similar to DF was encapsulated within the gliadin nanoparticles [35]. In detail, an EE% between ~10–20% was obtained when 0.05 and 0.1 mg/mL of rhodamine B were used, respectively, but when the same concentrations of DF were used, less than 2% of the hydrophilic compound was retained by the polymeric matrix. It should be noted that rhodamine B is characterized by a higher molecular weight than DF (479 g/mol vs. 376 g/mol) and significantly lower water solubility (15 g/L vs. 500 g/L). It is probable that the resulting EE is due to the lack of the diethylamino- and diethylazanium residues in the DF molecule. In addition, the occurrence of π -stacking interactions between the tryptophan residues of gliadin and the xanthene nucleus of rhodamine B could be another plausible interaction mechanism responsible for promoting the retention of this compound in the polymeric nanoparticles, as demonstrated in the case of poly (sodium 4-styrenesulfonate)- and poly (*N*-methacryloyl-5-aminoasalicic acid)-based nanosystems [59].

Contrarily, the gliadin nanoparticles prepared with BB allowed great retention of this compound; in particular, the highest EE% was obtained when an amount of 0.05 and 0.1 mg/mL of BB was used because ~50% of the compound initially added became entrapped within the nanosystems (Figure 2 and Table 3). But even though a slight decrease in the EE% was observed when higher amounts of the compound were initially used (47% and 43% for the samples prepared with 0.2 and 0.4 mg/mL of BB, respectively), there was a signifi-

cant increase in the LC% value, confirming a great affinity between this molecule and the polymeric structure.

4. Conclusions

The findings provided in this study demonstrate that the physico-chemical properties of a molecule dramatically influence its retention rate within gliadin nanoparticles as well as the sizing of the resulting systems.

In this regard, it is not suitable to make generalizations concerning the ability of an optimized nanoformulation to entrap compounds that share some common features such as solubility and/or structural conformation [56].

This is due to the fact that the entrapment efficiency is mainly affected by the molecular interactions occurring between the cargo molecule and the polymer [23,60]. This aspect has to be carefully taken into account during the phase of development of a new formulation to be used as a drug delivery system as a function of the required outcome, especially when a protein is the main component [61,62].

The delivery of hydrophilic compounds is a challenge for pharmaceutical technology because of the various drawbacks associated with their use, such as modest intracellular accumulation and rapid clearance [17,63]. Despite the intrinsic hydrophobicity of gliadin as a polymer, the proposed nanoparticles were shown to possess a good affinity for water-soluble compounds. In view of these results and considering the mucoadhesive features that characterize this biomaterial, besides the different plausible applications of the gliadin nanosystems (for example, delivery of bioactive compounds or development of novel nutraceuticals), the evaluation of the phenomena occurring at the interface of the protein will be fundamental for the refinement of the best formulations [64–68].

Author Contributions: Conceptualization, S.V. and D.C.; methodology, S.V.; software, S.V.; validation, S.V., M.F. and D.C.; formal analysis, S.V. and D.C.; resources, M.F. and D.C.; writing—original draft preparation, S.V.; writing—review and editing, S.V. and D.C.; funding acquisition, M.F. and D.C. All authors have read and agreed to the published version of the manuscript.

Funding: This research was funded by a grant from the Italian Ministry of University and Research (PRIN2017, prot. n. 20173ZECCM_003).

Data Availability Statement: The data presented in this study are available on request from the corresponding author.

Acknowledgments: The authors are very grateful to Lynn Whitted for her language revision of this article.

Conflicts of Interest: The authors declare no conflict of interest in this work.

References

1. Banik, B.L.; Fattahi, P.; Brown, J.L. Polymeric nanoparticles: The future of nanomedicine. *Wiley Interdiscip. Rev. Nanomed. Nanobiotechnol.* **2016**, *8*, 271–299. [[CrossRef](#)]
2. Palma, E.; Costa, N.; Molinaro, R.; Francardi, M.; Paolino, D.; Cosco, D.; Fresta, M. Improvement of the therapeutic treatment of inflammatory bowel diseases following rectal administration of mesalazine-loaded chitosan microparticles vs Asamax®. *Carbohydr. Polym.* **2019**, *212*, 430–438. [[CrossRef](#)] [[PubMed](#)]
3. Voci, S.; Gagliardi, A.; Fresta, M.; Cosco, D. Antitumor Features of Vegetal Protein-Based Nanotherapeutics. *Pharmaceutics* **2020**, *12*, 65. [[CrossRef](#)] [[PubMed](#)]
4. Voci, S.; Gagliardi, A.; Molinaro, R.; Fresta, M.; Cosco, D. Recent Advances of Taxol-Loaded Biocompatible Nanocarriers Embedded in Natural Polymer-Based Hydrogels. *Gels* **2021**, *7*, 33. [[CrossRef](#)]
5. Khalid, M.; El-Sawy, H.S. Polymeric nanoparticles: Promising platform for drug delivery. *Int. J. Pharm.* **2017**, *528*, 675–691. [[CrossRef](#)]
6. Thiruvengadam, M.; Rajakumar, G.; Chung, I.M. Nanotechnology: Current uses and future applications in the food industry. *Biotech* **2018**, *8*, 74. [[CrossRef](#)]
7. Gagliardi, A.; Giuliano, E.; Eeda, V.; Fresta, M.; Bulotta, S.; Awasthi, V.; Cosco, D. Biodegradable polymeric nanoparticles for drug delivery to solid tumors. *Front. Pharmacol.* **2021**, *12*, 17. [[CrossRef](#)]
8. Elzoghby, A.O.; Helmy, M.W.; Samy, W.M.; Elgindy, N.A. Novel ionically crosslinked casein nanoparticles for flutamide delivery: Formulation, characterization, and in vivo pharmacokinetics. *Int. J. Nanomed.* **2013**, *8*, 1721–1732. [[CrossRef](#)]

9. Jain, A.; Singh, S.K.; Arya, S.K.; Kundu, S.C.; Kapoor, S. Protein nanoparticles: Promising platforms for drug delivery applications. *ACS Biomater. Sci. Eng.* **2018**, *4*, 3939–3961. [[CrossRef](#)]
10. Martínez-López, A.L.; Pangua, C.; Reboredo, C.; Campión, R.; Morales-Gracia, J.; Irache, J.M. Protein-based nanoparticles for drug delivery purposes. *Int. J. Pharm.* **2020**, *581*, 119–289. [[CrossRef](#)] [[PubMed](#)]
11. Gagliardi, A.; Voci, S.; Bonacci, S.; Iriti, G.; Procopio, A.; Fresta, M.; Cosco, D. SCLAREIN (SCLAREol contained in zeIN) nanoparticles: Development and characterization of an innovative natural nanoformulation. *Int. J. Biol.* **2021**, *193*, 713–720. [[CrossRef](#)]
12. Irache, J.M.; González-Navarro, C.J. Zein nanoparticles as vehicles for oral delivery purposes. *Nanomedicine* **2017**, *12*, 1209–1211. [[CrossRef](#)]
13. Reboredo, C.; González-Navarro, C.J.; Martínez-Oharriz, C.; Martínez-López, A.L.; Irache, J.M. Preparation and evaluation of PEG-coated zein nanoparticles for oral drug delivery purposes. *Int. J. Pharm.* **2021**, *597*, 120–287. [[CrossRef](#)] [[PubMed](#)]
14. Zhu, X.; Chen, Y.; Hu, Y.; Han, Y.; Xu, J.; Zhao, Y.; Li, B. Tuning the molecular interactions between gliadin and tannic acid to prepare Pickering stabilizers with improved emulsifying properties. *Food Hydrocoll.* **2021**, *111*, 106–179. [[CrossRef](#)]
15. Caron, G.; Vallaro, M.; Ermondi, G. Log P as a tool in intramolecular hydrogen bond considerations. *Drug Discov. Today Technol.* **2018**, *27*, 65–70. [[CrossRef](#)] [[PubMed](#)]
16. Truzzi, F.; Tibaldi, C.; Zhang, Y.; Dinelli, G.; D’Amen, E. An Overview on Dietary Polyphenols and Their Biopharmaceutical Classification System (BCS). *Int. J. Mol. Sci.* **2021**, *22*, 5514. [[CrossRef](#)]
17. Vrignaud, S.; Benoit, J.P.; Saulnier, P. Strategies for the nanoencapsulation of hydrophilic molecules in polymer-based nanoparticles. *Biomaterials* **2011**, *32*, 8593–8604. [[CrossRef](#)]
18. Bharate, S.S.; Vishwakarma, R.A. Impact of preformulation on drug development. *Expert Opin. Drug Deliv.* **2013**, *10*, 1239–1257. [[CrossRef](#)]
19. Sohail, M.F.; Rehman, M.; Sarwar, H.S.; Naveed, S.; Salman, O.; Bukhari, N.I.; Shahnaz, G. Advancements in the oral delivery of Docetaxel: Challenges, current state-of-the-art and future trends. *Int. J. Nanomed.* **2018**, *13*, 3145. [[CrossRef](#)]
20. Patra, J.K.; Das, G.; Fraceto, L.F.; Campos, E.V.R.; del Pilar Rodriguez-Torres, M.; Acosta-Torres, L.S.; Shin, H.S. Nano based drug delivery systems: Recent developments and future prospects. *J. Nanobiotechnol.* **2018**, *16*, 1–33. [[CrossRef](#)]
21. Cosco, D.; Mare, R.; Paolino, D.; Salvatici, M.C.; Cilurzo, F.; Fresta, M. Sclareol-loaded hyaluronan-coated PLGA nanoparticles: Physico-chemical properties and in vitro anticancer features. *Int. J. Biol. Macromol.* **2019**, *132*, 550–557. [[CrossRef](#)] [[PubMed](#)]
22. Cosco, D.; Bruno, F.; Castelli, G.; Puleio, R.; Bonacci, S.; Procopio, A.; Paolino, D. Meglumine Antimoniate-Loaded Aqueous-Core PLA Nanocapsules: Old Drug, New Formulation against Leishmania-Related Diseases. *Macromol. Biosci.* **2021**, *2100046*. [[CrossRef](#)] [[PubMed](#)]
23. Gupta, S.; Singh, M.; Reddy, A.; Yavvari, P.S.; Srivastava, A.; Bajaj, A. Interactions governing the entrapment of anticancer drugs by low-molecular-weight hydrogelator for drug delivery applications. *RSC Adv.* **2016**, *6*, 19751–19757. [[CrossRef](#)]
24. Hoda, M.; Sufi, S.A.; Cavuturu, B.; Rajagopalan, R. Stabilizers influence drug–polymer interactions and physicochemical properties of disulfiram-loaded poly-lactide-co-glycolide nanoparticles. *Future Sci. OA* **2017**, *4*, 263. [[CrossRef](#)]
25. Redhead, H.M.; Davis, S.S.; Illum, L. Drug delivery in poly (lactide-co-glycolide) nanoparticles surface modified with poloxamer 407 and poloxamine 908: In vitro characterisation and in vivo evaluation. *J. Control. Rel.* **2001**, *70*, 353–363. [[CrossRef](#)]
26. He, H.; Zhang, J.; Xie, Y.; Lu, Y.; Qi, J.; Ahmad, E.; Wu, W. Bioimaging of intravenous polymeric micelles based on discrimination of integral particles using an environment-responsive probe. *Mol. Pharm.* **2016**, *13*, 4013–4019. [[CrossRef](#)] [[PubMed](#)]
27. Li, H.; Wang, K.; Yang, X.; Zhou, Y.; Ping, Q.; Oupicky, D.; Sun, M. Dual-function nanostructured lipid carriers to deliver IR780 for breast cancer treatment: Anti-metastatic and photothermal anti-tumor therapy. *Acta Biomater.* **2017**, *53*, 399–413. [[CrossRef](#)]
28. Trindade, I.C.; Pound-Lana, G.; Pereira, D.G.S.; de Oliveira, L.A.M.; Andrade, M.S.; Vilela, J.M.C.; Mosqueira, V.C.F. Mechanisms of interaction of biodegradable polyester nanocapsules with non-phagocytic cells. *Eur. J. Pharm. Sci.* **2018**, *124*, 89104. [[CrossRef](#)]
29. de Oliveira, M.A.; Pound-Lana, G.; Capelari-Oliveira, P.; Pontifice, T.G.; Silva, S.E.D.; Machado, M.G.C.; Mosqueira, V.C.F. Release, transfer and partition of fluorescent dyes from polymeric nanocarriers to serum proteins monitored by asymmetric flow field-flow fractionation. *J. Chromatogr. A* **2021**, *1641*, 461959. [[CrossRef](#)]
30. Wang, X.Y.; Koller, R.; Wirth, M.; Gabor, F. Lectin-grafted PLGA microcarriers loaded with fluorescent model drugs: Characteristics, release profiles, and cytoadhesion studies. *Sci. Pharm.* **2014**, *82*, 193–206. [[CrossRef](#)]
31. Gagliardi, A.; Voci, S.; Paolino, D.; Fresta, M.; Cosco, D. Influence of Various Model Compounds on the Rheological Properties of Zein-Based Gels. *Molecules* **2020**, *25*, 3174. [[CrossRef](#)]
32. Ahsan, N.; Siddique, I.A.; Gupta, S.; Surolia, A. A routinely used protein staining dye acts as an inhibitor of wild type and mutant alpha-synuclein aggregation and modulator of neurotoxicity. *Eur. J. Med. Chem.* **2018**, *143*, 1174–1184. [[CrossRef](#)]
33. Wang, L.; Wang, Y.; Han, Y.; Henderson, S.C.; Majeska, R.J.; Weinbaum, S.; Schaer, M.B. In situ measurement of solute transport in the bone lacunar-canalicular system. *Proc. Natl. Acad. Sci. USA* **2005**, *102*, 11911–11916. [[CrossRef](#)]
34. Gagliardi, A.; Paolino, D.; Costa, N.; Fresta, M.; Cosco, D. Zein-vs PLGA-based nanoparticles containing rutin: A comparative investigation. *Mater. Sci. Eng. C* **2021**, *118*, 111538. [[CrossRef](#)]
35. Voci, S.; Gagliardi, A.; Salvatici, M.C.; Fresta, M.; Cosco, D. Development of polyoxyethylene (2) oleyl ether-gliadin nanoparticles: Characterization and in vitro cytotoxicity. *Eur. J. Pharm. Sci.* **2021**, *162*, 105849. [[CrossRef](#)]
36. Gagliardi, A.; Cosco, D.; Udongo, B.P.; Dini, L.; Viglietto, G.; Paolino, D. Design and Characterization of Glyceryl Monooleate-Nanostructures Containing Doxorubicin Hydrochloride. *Pharmaceutics* **2020**, *12*, 1017. [[CrossRef](#)] [[PubMed](#)]

37. Gagliardi, A.; Voci, S.; Giuliano, E.; Salvatici, M.C.; Celano, M.; Fresta, M.; Cosco, D. Phospholipid/zein hybrid nanoparticles as promising carriers for the protection and delivery of all-trans retinoic acid. *Mater. Sci. Eng.* **2021**, *128*, 112331. [[CrossRef](#)] [[PubMed](#)]
38. Gagliardi, A.; Voci, S.; Salvatici, M.C.; Fresta, M.; Cosco, D. Brij-stabilized zein nanoparticles as potential drug carriers. *Colloids Surf. B* **2021**, *201*, 111647. [[CrossRef](#)] [[PubMed](#)]
39. Chen, S.; Ma, Y.; Dai, L.; Liao, W.; Zhang, L.; Liu, J.; Gao, Y. Fabrication, characterization, stability and re-dispersibility of curcumin-loaded gliadin-rhamnolipid composite nanoparticles using pH-driven method. *Food Hydrocoll.* **2021**, *118*, 106758. [[CrossRef](#)]
40. Gulfam, M.; Kim, J.E.; Lee, J.M.; Ku, B.; Chung, B.H.; Chung, B.G. Anticancer drug-loaded gliadin nanoparticles induce apoptosis in breast cancer cells. *Langmuir* **2012**, *28*, 8216–8223. [[CrossRef](#)]
41. Maity, M.; Dolui, S.; Maiti, N.C. Hydrogen bonding plays a significant role in the binding of coomassie brilliant blue-R to hemoglobin: FT-IR, fluorescence and molecular dynamics studies. *Phys. Chem. Chem. Phys.* **2015**, *17*, 31216–31227. [[CrossRef](#)]
42. Karthikeyan, K.; Vijayalakshmi, E.; Korrapati, P.S. Selective interactions of zein microspheres with different class of drugs: An in vitro and in silico analysis. *AAPS PharmSciTech* **2014**, *15*, 1172–1180. [[CrossRef](#)]
43. Davidov-Pardo, G.; Joye, I.J.; McClements, D.J. Encapsulation of resveratrol in biopolymer particles produced using liquid antisolvent precipitation. Part 1: Preparation and characterization. *Food Hydrocoll.* **2015**, *45*, 309–316. [[CrossRef](#)]
44. Liu, X.; Huang, Y.Q.; Chen, X.W.; Deng, Z.Y.; Yang, X.Q. Whole cereal protein-based Pickering emulsions prepared by zein-gliadin complex particles. *J. Cereal Sci.* **2019**, *87*, 46–51. [[CrossRef](#)]
45. Thewissen, B.G.; Celus, I.; Brijs, K.; Delcour, J.A. Foaming properties of wheat gliadin. *J. Agric. Food. Chem.* **2011**, *59*, 1370–1375. [[CrossRef](#)] [[PubMed](#)]
46. Voci, S.; Fresta, M.; Cosco, D. Gliadins as versatile biomaterials for drug delivery applications. *J. Control. Release* **2021**, *329*, 385–400. [[CrossRef](#)]
47. Luo, Y.; Pan, K.; Zhong, Q. Casein/pectin nanocomplexes as potential oral delivery vehicles. *Int. J. Pharm.* **2015**, *486*, 59–68. [[CrossRef](#)]
48. Klein, S.; Luchs, T.; Leng, A.; Distel, L.V.; Neuhuber, W.; Hirsch, A. Encapsulation of Hydrophobic Drugs in Shell-by-Shell Coated Nanoparticles for Radio—and Chemotherapy—An In Vitro Study. *Bioengineering* **2020**, *7*, 126. [[CrossRef](#)] [[PubMed](#)]
49. Majumder, D.; Roychoudhry, S.; Kundu, S.; Dey, S.K.; Saha, C. Hydrophobic quercetin encapsulated hemoglobin nanoparticles: Formulation and spectroscopic characterization. *J. Biomol. Struct. Dyn.* **2021**, 1–10. [[CrossRef](#)]
50. Das, S.; Bora, N.; Rohman, M.A.; Sharma, R.; Jha, A.N.; Roy, A.S. Molecular recognition of bio-active flavonoids quercetin and rutin by bovine hemoglobin: An overview of the binding mechanism, thermodynamics and structural aspects through multi-spectroscopic and molecular dynamics simulation studies. *Phys. Chem. Chem. Phys.* **2018**, *20*, 21668–21684. [[CrossRef](#)]
51. Herrera, M.G.; Veuthey, T.V.; Dodero, V.I. Self-organization of gliadin in aqueous media under physiological digestive pHs. *Colloids Surf. B Biointerfaces* **2016**, *141*, 565–575. [[CrossRef](#)]
52. Wouters, A.G.; Schaefer, S.; Joye, I.J.; Delcour, J.A. Relating the structural, air-water interfacial and foaming properties of wheat (*Triticum aestivum* L.) gliadin and maize (*Zea mays* L.) zein based nanoparticle suspensions. *Colloids Surf. A Physicochem. Eng. Asp.* **2019**, *567*, 249–259. [[CrossRef](#)]
53. Fang, R.; Jing, H.; Chai, Z.; Zhao, G.; Stoll, S.; Ren, F.; Leng, X. Study of the physicochemical properties of the BSA: Flavonoid nanoparticle. *Eur. Food Res. Technol.* **2011**, *233*, 275–283. [[CrossRef](#)]
54. Sengupta, P.; Sardar, P.S.; Roy, P.; Dasgupta, S.; Bose, A. Investigation on the interaction of Rutin with serum albumins: Insights from spectroscopic and molecular docking techniques. *J. Photochem. Photobiol. B Biol.* **2018**, *183*, 101–110. [[CrossRef](#)]
55. Rawel, H.M.; Rohn, S.; Kroll, J. Influence of a sugar moiety (rhamnosylglucoside) at 3-O position on the reactivity of quercetin with whey proteins. *Int. J. Biol. Macromol.* **2003**, *32*, 109–120. [[CrossRef](#)]
56. Luo, Y. Perspectives on important considerations in designing nanoparticles for oral delivery applications in food. *J. Agric. Food Inf.* **2020**, *2*, 100031. [[CrossRef](#)]
57. Gutiérrez-Valenzuela, C.A.; Esquivel, R.; Guerrero-Germán, P.; Zavala-Rivera, P.; Rodríguez-Figueroa, J.C.; Guzmán-Z, R.; Lucero-Acuña, A. Evaluation of a combined emulsion process to encapsulate methylene blue into PLGA nanoparticles. *RSC Adv.* **2018**, *8*, 414–422. [[CrossRef](#)]
58. Barbero, N.; Barni, E.; Barolo, C.; Quagliotto, P.; Viscardi, G.; Napione, L.; Bussolino, F. A study of the interaction between fluorescein sodium salt and bovine serum albumin by steady-state fluorescence. *Dyes Pigm.* **2009**, *80*, 307–313. [[CrossRef](#)]
59. Moreno-Villoslada, I.; Jofré, M.; Miranda, V.; Chandía, P.; González, R.; Hess, S.; Nishide, H. π -Stacking of rhodamine B onto water-soluble polymers containing aromatic groups. *Polymer* **2006**, *47*, 6496–6500. [[CrossRef](#)]
60. Lv, S.; Wu, Y.; Cai, K.; He, H.; Li, Y.; Lan, M.; Yin, L. High drug loading and sub-quantitative loading efficiency of polymeric micelles driven by donor-receptor coordination interactions. *J. Am. Chem. Soc.* **2018**, *140*, 1235–1238. [[CrossRef](#)]
61. McClements, D.J. Encapsulation, protection, and release of hydrophilic active components: Potential and limitations of colloidal delivery systems. *Adv. Colloid Interface Sci.* **2015**, *219*, 27–53. [[CrossRef](#)] [[PubMed](#)]
62. Mohammadian, M.; Waly, M.I.; Moghadam, M.; Emam-Djomeh, Z.; Salami, M.; Moosavi-Movahedi, A.A. Nanostructured food proteins as efficient systems for the encapsulation of bioactive compounds. *Food Sci. Hum. Wellness* **2020**, *9*, 199–213. [[CrossRef](#)]
63. Arpicco, S.; Battaglia, L.; Brusa, P.; Cavalli, R.; Chirio, D.; Dosio, F.; Ceruti, M. Recent studies on the delivery of hydrophilic drugs in nanoparticulate systems. *J. Drug. Deliv. Sci. Technol.* **2016**, *32*, 298–312. [[CrossRef](#)]

64. Sharma, K.; Deevenapalli, M.; Singh, D.; Chourasia, M.K.; Bathula, S.R. Preparation and characterization of paclitaxel-loaded gliadin nanoparticles. *J. Biomater. Tissue Eng.* **2014**, *4*, 399–404. [[CrossRef](#)]
65. Sonekar, S.; Mishra, M.K.; Patel, A.K.; Nair, S.K.; Singh, C.S.; Singh, A.K. Formulation and evaluation of folic acid conjugated gliadin nanoparticles of curcumin for targeting colon cancer cells. *J. Appl. Pharm. Sci.* **2016**, *6*, 68–74. [[CrossRef](#)]
66. Joye, I.J.; Davidov-Pardo, G.; McClements, D.J. Encapsulation of resveratrol in biopolymer particles produced using liquid antisolvent precipitation. Part 2: Stability and functionality. *Food Hydrocoll.* **2015**, *49*, 127–134. [[CrossRef](#)]
67. Abdelmoneem, M.A.; Mahmoud, M.; Zaky, A.; Helmy, M.W.; Sallam, M.; Fang, J.Y.; Elzoghby, A.O. Decorating protein nanospheres with lactoferrin enhances oral COX-2 inhibitor/herbal therapy of hepatocellular carcinoma. *Nanomedicine* **2018**, *13*, 2377–2395. [[CrossRef](#)]
68. He, J.R.; Zhu, J.J.; Yin, S.W.; Yang, X.Q. Bioaccessibility and intracellular antioxidant activity of phloretin embodied by gliadin/sodium carboxymethyl cellulose nanoparticles. *Food Hydrocoll.* **2022**, *122*, 107076. [[CrossRef](#)]